Derivation of a master equation for charge-transfer processes in atom-surface collisions

David C. Langreth
Department of Physics and Astronomy, Rutgers University, Piscataway, New Jersey 08855-0849

P. Nordlander
Department of Physics and Rice Quantum Institute, Rice University, Houston, Texas 77251-1892
(Received 13 August 1990)

The time-dependent Anderson model for multiple levels interacting with a continuum is studied using the slave-boson Green's-function technique, with an eye to understanding charge-transfer phenomena for an atomic species moving outside a metallic surface. It is shown that in the finite-temperature and low-velocity limit, the equations for the occupation numbers satisfy a master equation. Application to charge-exchange processes in atom-surface-scattering experiments shows that the presence of strong intra-atomic correlation effects can drastically change the charge-transfer dynamics.

I. INTRODUCTION

Charge-transfer processes play an important role for many dynamical phenomena at surfaces.[1-3] The probabilities for charge transfer were first calculated[4-8] with use of the time-dependent Anderson model. However, most treatments of charge-transfer reactions have neglected spin effects and the effects of intra-atomic Coulomb correlations. Some attempts to describe such effects in special limits have been performed,[9-13] but no systematic method for including intra-atomic correlation effects has been developed to date. These correlations are not small, and therefore cannot be treated by perturbation theory.

On the other hand, there has been much progress in highly correlated bulk problems which are normally described by the Anderson model. One method of systematically treating the large-U problem has been developed by Coleman,[14] who introduced "slave bosons" to replace the awkward projection operators that had been used in many previous treatments of the mixed-valence problem. Here, we adapt the slave-boson method to the time-dependent problem, and use it to show that the intra-atomic correlation effects can drastically alter the charge-transfer dynamics even for degenerate levels.

The theoretical description of electron transfer is complicated by interference effects and the solution for the electron coordinates is normally much more complicated than the solution for the nuclear coordinates. Nevertheless, considerable success has been obtained by combining realistic trajectory calculations with simple rate equations for describing survival rates and charge-transfer processes.

In this article, a method introduced by Kadanoff and Baym[15] is used to derive a rate equation of motion for a tunneling electron. This method is particularly useful in the current context since the structure of the Dyson equation (or more precisely the difference between two Dyson equations) resembles a master equation.[16] We show that under certain circumstances the dynamics of the electronic processes is well described by a very simple master equation, even in the presence of the strong Coulomb correlations mentioned earlier. This finding has potentially large importance since it enables the description of electron coordinates on the same level as nuclear coordinates and thus readily can be incorporated in trajectory or molecular dynamics simulations.

We show that the intra-atomic correlation effects can combine to prevent neutralization even though there are excited levels that are readily available for resonant neutralization. This mechanism provides a channel for the survival of hyperthermal positive ions in desorption and sputtering experiments.

In the sections that follow, we begin by showing how the Kadanoff-Baym formalism can be applied to derive master equations for the uncorrelated or $U = 0$ case. We do this first in the so-called semiclassical approximation, and obtain a simple intuitive master equation. We then derive the full or exact master equation for the $U = 0$ case. The exact equation can then be used to determine the precise region of validity of the approximation. Next we show how the slave-boson technique can be used in a parallel development for the highly correlated large-U case. First, we derive a master equation in the semiclassical approximation, and then make a better treatment which in turn can be used to find the region of validity of the simpler semiclassical treatment.

In Sec. II, we present the general method for deriving master equations, both in the $U = 0$ or single-level case, and in the $U = \infty$ multiple-level case. In Sec. III, we carry the program mentioned in the above paragraph, deriving semiclassical and exact or more exact master

equations in the respective cases. In Sec. IV, we present the numerical solutions of both our sets of master equations. We compare the results of the $U = 0$ and $U = \infty$ treatments in several situations that correspond to physical experiments. We find that the neglect of U as done in most previous treatments gives qualitatively incorrect results.

We suggest that future treatments use the master equation developed here for the correlated system. It is as easy to apply as the existing theory for the uncorrelated system.

II. GENERAL DERIVATION OF A MASTER EQUATION

A. Single-level case

Here we suppose that the atom moving outside the metallic surface has a single valence level of a particular spin which is allowed to mix as a function of time with the electronic states of the same spin in the substrate. It is assumed that neither other levels nor other spin occupations of the spatial level in question have any effect on the time-dependent occupations of the level in question. This is the "standard" way to approximate the physical problem, which has been applied many times before in the literature. As we will show later, it can be qualitatively incorrect, when the intra-atomic Coulomb interaction becomes substantial. We present it here to illustrate our master equation method, which in the next subsection is then applied to the more realistic case where there exist strong correlations induced by the intra-atomic Coulomb interaction.

The simple case discussed in this subsection can be described by a time-dependent resonant level model for a single impurity level. The "impurity" level is in this case taken to be the relevant level of the atomic species moving outside the surface. This Hamiltonian takes the form

$$H(t) = \varepsilon_a(t) n_a(t) + \sum_k \varepsilon_k n_k(t) + \sum_k V_{ak}(t) c_a^\dagger(t) c_k(t) + \text{H.c.} \tag{2.1}$$

In this expression, $\varepsilon_a(t)$ is the energy of the impurity level, ε_k the energies of the continuum eigenstates, and $V_{ak}(t)$ is the hopping matrix element between the impurity and the continuum states inside the metal.

Our aim is to derive master equations for the occupation of the impurity level. A rigorous and well established way to derive such equations was introduced by Kadanoff and Baym,[15] and has been applied to a number of different systems—see Langreth[16] for a review. This method develops exact equations for double-time Green's function $G(t,t')$, which in our case equals

$$iG(t,t') = \langle T c_a(t) c_a^\dagger(t') \rangle, \tag{2.2}$$

or more accurately equations for its analytic pieces $G^>(t,t')$ and $G^<(t,t')$ given by

$$iG(t,t') = G^>(t,t')\Theta(t-t') - G^<(t,t')\Theta(t'-t). \tag{2.3}$$

Here the time ordering operator T and the step functions Θ operate along a contour c in the complex plane. It will not matter in the presentation given here whether c is taken to be the Kadanoff-Baym contour, the Keldysh contour,[17] or a more general choice.[16]

The basic starting equations follow directly from the Dyson equations in time space for G:

$$\left(i\frac{\partial}{\partial t} - \varepsilon_a(t) \right) G(t,t') = \delta(t-t') + \int_c d\bar{t}\, \Sigma(t,\bar{t}) G(\bar{t},t') , \tag{2.4}$$

$$\left(-i\frac{\partial}{\partial t'} - \varepsilon_a(t') \right) G(t,t') = \delta(t-t') + \int_c d\bar{t}\, G(t,\bar{t}) \Sigma(\bar{t},t') , \tag{2.5}$$

plus an approximation (in this particular case an exact expression) for the self-energy Σ, and hence for its analytic pieces $\Sigma^>$ and $\Sigma^<$ defined analogously to $G^>$ and $G^<$ [i.e., symbolically replace G with Σ in (2.2)]. By using a set of identities[18,16] [see Appendix A] Eqs. (2.4) and (2.5) are readily continued to corresponding equations for the physical real-time correlation functions $G^<(t,t')$ and $G^>(t,t')$, whose equal time values, respectively, represent the number of electrons or holes in the impurity level as a function of time. These real-time equations for $G^<$ are

$$\left(i\frac{\partial}{\partial t} - \varepsilon_a(t) \right) G^<(t,t') = \int_{-\infty}^{\infty} d\bar{t}\, \left[\Sigma^R(t,\bar{t}) G^<(\bar{t},t') + \Sigma^<(t,\bar{t}) G^A(\bar{t},t') \right] , \tag{2.6}$$

$$\left(-i\frac{\partial}{\partial t'} - \varepsilon_a(t') \right) G^<(t,t') = \int_{-\infty}^{\infty} d\bar{t}\, \left[G^R(t,\bar{t}) \Sigma^<(\bar{t},t') + G^<(t,\bar{t}) \Sigma^A(\bar{t},t') \right] , \tag{2.7}$$

where G^R and G^A are the advanced and retarded Green's functions

$$\begin{aligned} iG^R(t,t') &= \left[G^>(t,t') + G^<(t,t') \right] \Theta(t-t') , \\ -iG^A(t,t') &= \left[G^>(t,t') + G^<(t,t') \right] \Theta(t'-t) , \end{aligned} \tag{2.8}$$

with analogous equations for Σ^R and Σ^A. In general there will be two equations for each "greater than" or "lesser than" quantity, as in (2.4) and (2.5), and hence (2.6) and (2.7); the right side of one can be symbolically obtained from the right side of the other other by switch-

ing the order of G and Σ and switching the advanced and retarded labels. To save space, we shall from now on only write one such equation, and simply refer to the other as its *conjugate* equation.

The G^A may be obtained by solving a traditional sort of real-time Dyson equation:

$$\left(i\frac{\partial}{\partial t}-\varepsilon_a(t)\right)G^A(t,t') = \delta(t-t')+\int_{-\infty}^{\infty}d\bar{t}\,\Sigma^A(t,\bar{t})G^A(\bar{t},t')\ , \quad (2.9)$$

along with the boundary condition that $G^A(t,t')=0$ for $t>t'$, while G^R satisfies an identical equation with the boundary condition that $G^R(t,t')=0$ for $t<t'$.

To close the above set of equations, one needs an approximate expression for Σ. The resonant level model, however, has no Coulomb correlations, and hence an exact expression is in principle possible:

$$\Sigma(t,t')=V_{ak}(t)g^{(0)}_{kk'}(t,t')V_{ak}(t')\ , \quad (2.10)$$

where $g^{(0)}$ is the *unperturbed* Green's function for the substrate electrons. For simplicity it is assumed that the hopping matrix element is separable, i.e., $V_{ak}(t)=V_k u(t)$ and that the density of free electron states ρ times the square of the potential V is a constant function of the energy ε corresponding to the quantum number k. With these simplifications we can write for the "greater than" or "lesser than" components of the self-energy

$$\Sigma^{\gtrless}(t,t')=u(t)u(t')\rho V^2\int_{-D}^{D}d\varepsilon\, f^{\gtrless}(\varepsilon)e^{-i\varepsilon(t-t')}, \quad (2.11)$$

where $f^<(\varepsilon)$ is the Fermi function, $f^>(\varepsilon)=1-f^<(\varepsilon)$, and D is the bandwidth, which we take to be infinite, except where it is needed for convergence. The latter approximations are not needed if we also make the so-called semiclassical approximation (SCA). Since one of the results of this work is that the semiclassical approximation is often a very good one, we will discuss at a later point the form of this solution without them.

In the wide band limit ($D\to\infty$), the integration over energy can be performed analytically and the self-energies take the form

$$\Sigma^{\gtrless}(t,t')=\sqrt{\Gamma(t)\Gamma(t')}\,f^{\gtrless}(t-t')\ , \quad (2.12)$$

where

$$\Gamma(t)=2\pi u^2(t)V^2\rho\ , \quad (2.13)$$

and where the functions $f^{\gtrless}(\tau)$ are the Fourier transforms

$$f^{\gtrless}(\tau)=\int_{-\infty}^{\infty}\frac{d\varepsilon}{2\pi}f^{\gtrless}(\varepsilon)e^{-i\varepsilon\tau}\ . \quad (2.14)$$

These can be readily evaluated to yield

$$f^<(\tau)=[f^>(\tau)]^*=\tfrac{1}{2}\delta(\tau)+\frac{ie^{-i\varepsilon_F\tau}}{2\beta\sinh\frac{\pi\tau}{\beta}}, \quad (2.15)$$

where ε_F is the Fermi energy.

The retarded and advanced self-energies can for this case be obtained straightforwardly from Eq. (2.12) and take the form

$$\Sigma^R(t,t')=[\Sigma^A(t',t)]^*=-i\Gamma(t)\delta(t-t')\Theta(t-t') =-\tfrac{1}{2}i\Gamma(t)\delta(t-t')\ . \quad (2.16)$$

The substitution of these expressions into Eq. (2.9) gives the following result for the retarded and advanced Green's functions:

$$G^A(t,t')=[G^R(t',t)]^* =-\frac{1}{i}\exp\left(-i\int_{t'}^{t}d\bar{t}\,[\varepsilon(\bar{t})+\tfrac{1}{2}i\Gamma(\bar{t})]\right)\Theta(t'-t)\ . \quad (2.17)$$

These expressions can be inserted directly in Eq. (2.6) and the occupation of level $|a\rangle$ can be calculated from the expression $n_a(t)=G^<(t,t)$. We discuss the solution of these equations in a later section.

B. Multiple levels interacting with a continuum

We now turn to the case of multiple levels interacting with a continuum. Because of spin degeneracy, even the simplest examples that describe physical reality fall into this category. The controlling difference between this case and the case considered in the previous subsection is that the intra-atomic Coulomb interaction between the electrons of the atomic species outside the surface is normally large and cannot be neglected. Thus instead of the exactly soluble resonant level model, one must deal with the time-dependent Anderson model instead:

$$H(t)=\sum_{\sigma}\varepsilon_\sigma(t)n_\sigma(t)+\tfrac{1}{2}\sum_{\sigma_1\neq\sigma_2}U_{\sigma_1\sigma_2}n_{\sigma_1}(t)n_{\sigma_2}(t) +\sum_k\varepsilon_k(t)n_k(t)+\sum_{\sigma k}[V_{\sigma k}(t)c_k^\dagger(t)c_\sigma(t)+\text{H.c.}]\ . \quad (2.18)$$

Here σ labels both the spin and spatial quantum numbers of the atomic orbitals, while k labels the spin and spatial quantum numbers of the solid. The solution of this Hamiltonian is complicated by the presence of the intra-atomic correlation term U. In the limit of large U, the effect of the correlation term is to restrict the occupation of the impurity levels to a maximum of one. In this context, large U means that $\varepsilon_\sigma+U\gg\varepsilon_F+kT$ and $\varepsilon_\sigma+U\gg\varepsilon_F+\Gamma$. These conditions are typically satisfied for excited neutral, ionization, and affinity levels of atoms interacting with metals. This large-U limit can be effected with the use of projection operators. This procedure has the disadvantage that a conventional Green's-function approach is complicated since these operators do not satisfy standard commutation relations. An alternative method for the equilibrium case (no time dependence) was suggested by Coleman[14] and has since been widely used. Here we adapt it to the time-dependent problem. In this method, a boson operator is introduced

in the term describing the hopping between the adsorbate level and the continuum. The slave-boson Hamiltonian takes the form

$$H(t) = \sum_\sigma \varepsilon_\sigma(t) n_\sigma(t) + \sum_k \varepsilon_k(t) n_k(t) + \sum_{\sigma k} [V_{\sigma k}(t) c_k^\dagger(t) c_\sigma(t) b^\dagger(t) + \text{H.c.}] \ . \quad (2.19)$$

When an electron tunnels into the metal, it creates a boson, and vice versa. The sum of the impurity occupation number and the slave-boson occupation number, $Q_B(t) = \sum_\sigma n_\sigma(t) + n_B(t)$, is conserved, where we have let $n_B(t) = b^\dagger(t) b(t)$. The diagonalization of the Hamiltonian is performed in the subspace of the Hilbert space containing the proper generalized occupation number Q_B, and the intra-atomic correlation term can thus be dropped. Since the boson operator is a conventional field operator, a standard perturbative expansion can be performed and a self-energy and a Dyson equation can be defined.

The self-energies for the impurity propagators and the slave-boson propagator have a straightforward perturbation expansion in powers of the hopping matrix element, as illustrated diagrammatically in Fig. 1. The Hamiltonian (2.19) is very rich and includes among other phenomena the Kondo problem and the mixed-valence problem as special cases. A simple exact solution as in the single-level case cannot therefore be hoped for; we represent the self-energies to lowest order in the hopping matrix element, thus keeping only the term which is directly analogous to that obtained in the single-level case:

$$\Sigma_\sigma^{\gtrless}(t,t') = \sqrt{\Gamma_\sigma(t)\Gamma_\sigma(t')}\, f^{\gtrless}(t-t') B^{\gtrless}(t,t'), \quad (2.20)$$

where $B^{\gtrless}$ are the analytic pieces of the slave-boson propagator:

$$iB(t,t') \equiv \langle T b(t) b^\dagger(t') \rangle = B^>(t,t')\Theta(t-t') + B^<(t,t')\Theta(t-t'). \quad (2.21)$$

Eq. (2.20) is thus analogous to Eq. (2.12) for the single-level case. We note that B is in principle the full self-consistent slave-boson propagator. Coleman[14] has shown for the case of n degenerate levels in thermal equilibrium, that when (2.20) and (2.21) are inserted into the appropriate Dyson equations, one obtains a result accurate to order $1/n^2$. Of course, to lowest order in V, these equations are exact. We also define retarded and advanced functions for the slave boson

$$B^R(t,t') = -i\,[B^>(t,t') - B^<(t,t')]\,\Theta(t-t') \ , \quad B^A(t,t') = i\,[B^>(t,t') - B^<(t,t')]\,\Theta(t'-t) \ . \quad (2.22)$$

The sign differences between this and (2.9) arise from the difference between boson and fermion commutation relations.

In applying the slave-boson method, one must project onto the subspace in which $Q_B = 1$. This is normally accomplished in the time-independent case by introducing a chemical potential associated with Q_B and then letting it approach $-\infty$ to achieve the low-density limit in this variable. The same effect is accomplished here by identifying the Q_B dependence of the various quantities, and then throwing away terms that are proportional to Q_B to higher than the lowest order. We do this by noting that $G^<$ and $B^<$ are proportional to $(Q_B)^1$, while G^A, G^R, B^A, and B^R are proportional to $(Q_B)^0$. Since the Dyson equations for $G^<$ will involve either $G^<$ or $B^<$ in every term, the self-energies that multiply these quantities must have all terms proportional to $(Q_B)^1$ or higher projected out. We emphasize that the omission of these terms is *not* an additional approximation, but is rather a projection technique that is *required* by slave-boson formulation of the problem. As a result we obtain from the diagrams of Fig. 1, the advanced and retarded self-energies

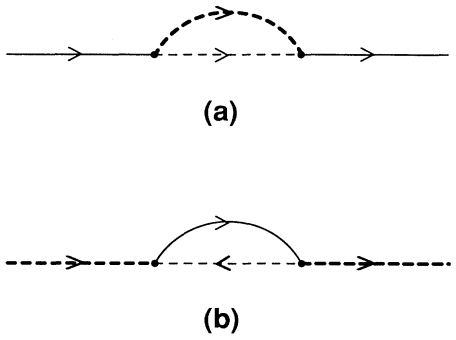

FIG. 1. Diagrammatic representation of the self-energy of (a) the atomic level propagator and (b) the slave-boson propagator. The solid line is the full propagator of the atomic level, the light dashed line is the conduction electron propagator, and the heavy dashed line is the fully interacting propagator for the slave boson.

$$\Sigma_\sigma^R(t,t') = \sqrt{\Gamma_\sigma(t)\Gamma_\sigma(t')}\, f^>(t-t') B^R(t,t') \ , \quad \Sigma_\sigma^A(t,t') = \sqrt{\Gamma_\sigma(t)\Gamma_\sigma(t')}\, f^>(t-t') B^A(t,t') \ , \quad (2.23)$$

for the electron propagator, and

$$\Pi^R(t,t') = \sum_\sigma \sqrt{\Gamma_\sigma(t)\Gamma_\sigma(t')}\, f^<(t-t') G_\sigma^R(t,t') \ , \quad \Pi^A(t,t') = \sum_\sigma \sqrt{\Gamma_\sigma(t)\Gamma_\sigma(t')}\, f^<(t-t') G_\sigma^A(t,t') \ , \quad (2.24)$$

for the boson propagator. In the time-independent limit, Eqs. (2.24) and (2.25) become identical to the constant $V^2\rho$ limit of Coleman's[14] equation (A4). The Dyson equation for $G^<(t,t')$ then takes the form

$$\left(i\frac{\partial}{\partial t}-\varepsilon_\sigma(t)\right)G_\sigma^<(t,t')=\int_{-\infty}^{\infty}d\bar{t}\,\sqrt{\Gamma_\sigma(t)\Gamma_\sigma(\bar{t})}\,f^>(t-\bar{t})B^R(t,\bar{t})G_\sigma^<(\bar{t},t')+\int_{-\infty}^{\infty}d\bar{t}\,\sqrt{\Gamma_\sigma(t)\Gamma_\sigma(\bar{t})}\,f^<(t-\bar{t})B^<(t,\bar{t})G_\sigma^A(\bar{t},t')\ . \tag{2.25}$$

Similarly, the Dyson equation for the boson propagator is

$$i\frac{\partial}{\partial t}B^<(t,t')=\sum_\sigma\int_{-\infty}^{\infty}d\bar{t}\,\sqrt{\Gamma_\sigma(t)\Gamma_\sigma(\bar{t})}\,f^<(\bar{t}-t)G_\sigma^R(t,\bar{t})B^<(\bar{t},t')+\sum_\sigma\int_{-\infty}^{\infty}d\bar{t}\,\sqrt{\Gamma_\sigma(t)\Gamma_\sigma(\bar{t})}\,f^>(\bar{t}-t)G_\sigma^<(t,\bar{t})B^A(\bar{t},t'). \tag{2.26}$$

Finally, the retarded Green's functions satisfy

$$\left(i\frac{\partial}{\partial t}-\varepsilon_\sigma(t)\right)G_\sigma^R(t,t')=\delta(t-t')+\int_{-\infty}^{\infty}d\bar{t}\,\sqrt{\Gamma_\sigma(t)\Gamma_\sigma(\bar{t})}\,f^>(t-\bar{t})B^R(t,\bar{t})G^R(\bar{t},t') \tag{2.27}$$

for the impurity, and

$$i\frac{\partial}{\partial t}B^R(t,t')=\delta(t-t')+\sum_\sigma\int_{-\infty}^{\infty}d\bar{t}\,\sqrt{\Gamma_\sigma(t)\Gamma_\sigma(\bar{t})}\,f^<(\bar{t}-t)G_\sigma^R(t,\bar{t})B^R(\bar{t},t') \tag{2.28}$$

for the boson. From the solution of these equations, one can calculate $n_\sigma(t)\equiv G_\sigma^<(t,t)$ as a function of t. The boson Hamiltonian ensures that Q_B is conserved, while the projection technique ensures that it is unity. The unphysical states with $\sum_\sigma n_\sigma>1$ can never become occupied if they were unoccupied at $t=-\infty$, so that $n_\sigma(t)$ is the time-dependent occupation number of the level $|\sigma\rangle$ just as in the single-level case. One can ensure that this is true simply by taking $\varepsilon_\sigma(-\infty)\to\infty$.

III. SEMICLASSICAL APPROXIMATION AND BEYOND

The equations derived in the last section are rather cumbersome. For low velocities and for $U=0$, it has been demonstrated that certain approximations can be made and that a classical master equation can result.[19,8] In this section, we further investigate the conditions under which a semiclassical approximation results. We will show how the Dyson equations for the Green's functions reduce to simple master equations for the occupations of the levels.

A. U=0 limit

The Dyson equation for the $U=0$ case was derived in the previous section—see Eq. (2.6). It is convenient to factor out the oscillatory part of the Green functions. We thus write

$$\tilde{G}(t,t')=G(t,t')\exp\left(i\int_{t'}^{t}d\tau\,\varepsilon_a(\tau)\right) \tag{3.1}$$

for the respective Green function and

$$\tilde{f}^{\gtrless}(t,t')=f^{\gtrless}(t-t')\exp\left(i\int_{t'}^{t}d\tau\,\varepsilon_a(\tau)\right) \tag{3.2}$$

for the functions $f^{\gtrless}$ used in the self-energies. The Dyson equation then takes the form

$$i\frac{\partial}{\partial t}\tilde{G}^<(t,t')=-i\frac{\Gamma(t)}{2}\tilde{G}^<(t,t')+\int_{-\infty}^{\infty}d\bar{t}\,\sqrt{\Gamma(t)\Gamma(\bar{t})}\,\tilde{f}^<(t,\bar{t})\tilde{G}^A(\bar{t},t')\ . \tag{3.3}$$

In the wide band limit, the real part of the functions $\tilde{f}^{\gtrless}$ take the form

$$\mathrm{Re}\,\tilde{f}^<(t,t')=\tfrac{1}{2}\delta(t-t')-\frac{\sin\int_{t'}^{t}d\tau[\varepsilon_a(\tau)-\varepsilon_F]}{2\beta\sinh\frac{\pi(t-t')}{\beta}}\ , \tag{3.4}$$

$$\mathrm{Re}\,\tilde{f}^>(t,t')=\tfrac{1}{2}\delta(t-t')+\frac{\sin\int_{t'}^{t}d\tau[\varepsilon_a(\tau)-\varepsilon_F]}{2\beta\sinh\frac{\pi(t-t')}{\beta}}\ .$$

One would have to restore the bandwidth cutoff D when $t\approx t'$ in the imaginary parts of $\tilde{f}^{\gtrless}$, but these imaginary parts cancel out and do not contribute to the single-level or $U=0$ problem.

It can be seen that these functions are localized around equal time. In particular, this will be the case for large temperatures. We can immediately conclude therefore, that in the high-temperature limit the semiclassical approximation will be valid provided $\varepsilon_a\neq\varepsilon_F$. There is also a localization due to the rapidly varying phase in the numerator. In Appendix B we present a detailed discussion of the criteria of validity of the SCA.

The semiclassical approximation (SCA) results when the functions $\tilde{f}^{\gtrless}$ are sufficiently peaked around equal times $\bar{t}=t$ that the Green's functions and $\sqrt{\Gamma(\bar{t})}$ can be taken outside the integral, i.e.

$$\int_{-\infty}^{\infty}d\bar{t}\,\sqrt{\Gamma(t)\Gamma(\bar{t})}\,\mathrm{Re}[\tilde{f}^<(t,\bar{t})]\tilde{G}^A(\bar{t},t')\approx\Gamma(t)\tilde{G}^A(t,t')\int_{-\infty}^{t'}d\bar{t}\,\mathrm{Re}[\tilde{f}^<(t,\bar{t})]\ . \tag{3.5}$$

The resulting integrals (3.5), can then directly be evaluated and in Appendix B it is shown that these integrals are well approximated by the Fermi function:

$$\int_{-\infty}^{t} d\bar{t}\, \tilde{f}^{\gtrless}(t,\bar{t}) \approx \tfrac{1}{2} f^{\gtrless}(\varepsilon_a(t)) \ . \tag{3.6}$$

Using the relation

$$\frac{d}{dt} n_a(t) = \frac{\partial}{\partial t} G^{<}(t,t')\Big|_{t=t'} + \frac{\partial}{\partial t'} G^{<}(t,t')\Big|_{t=t'} \tag{3.7}$$

along with the approximations (3.5) and (3.6) allows us to obtain an equation for the occupation of level $|a\rangle$ by adding (3.3) to its conjugate, and we obtain

$$\frac{d}{dt} n_a(t) = -\Gamma(t) n_a(t) + f^{<}(\varepsilon_a(t))\Gamma(t). \tag{3.8}$$

This master equation can readily be solved. It can also be easily derived by intuitive golden rule considerations.

The quality of the SCA for $U = 0$ can directly be tested, since in the wide band limit the retarded and advanced Green's functions are analytical. Using the expression (2.16) for the self-energies in the Dyson equation (2.9), one finds that

$$i\frac{\partial}{\partial t}\tilde{G}^{A}(t,t') = \delta(t-t') + i\frac{\Gamma(t)}{2}\tilde{G}^{A}(t,t') \ . \tag{3.9}$$

This equation can directly be solved, yielding

$$\tilde{G}^{A}(t,t') = i\Theta(t'-t)\exp\int_{t'}^{t} d\tau\, \frac{\Gamma(\tau)}{2}. \tag{3.10}$$

This expression can now be substituted into Eq. (3.3) and the exact equation for the charge transfer becomes

$$\frac{d}{dt} n_a(t) = -\Gamma(t) n_a(t) + 2\,\mathrm{Re}\int_{-\infty}^{t} d\bar{t}\, \sqrt{\Gamma(t)\Gamma(\bar{t})}\, \tilde{f}^{<}(t,\bar{t}) \exp\left(-\int_{\bar{t}}^{t} d\tau\, \frac{\Gamma(\tau)}{2}\right) \ . \tag{3.11}$$

This equation can be written in terms of a function $c(t)$ that describes the accuracy of the approximation Eq. (3.5):

$$\frac{d}{dt} n_a(t) = -\Gamma(t) n_a(t) + \Gamma(t) f(\varepsilon_a(t)) + \Gamma(t) c(t) \ . \tag{3.12}$$

The expression for the function $c(t)$ is

$$\begin{aligned} c(t) &= \frac{2}{\Gamma(t)}\mathrm{Re}\int_{-\infty}^{t} d\bar{t}\, \sqrt{\Gamma(t)\Gamma(\bar{t})}\, \tilde{f}^{<}(t,\bar{t}) \exp\left(-\int_{\bar{t}}^{t} d\tau\, \frac{\Gamma(\tau)}{2}\right) - f^{<}(\varepsilon_a(t)) \\ &= -\int_{-\infty}^{t} d\bar{t}\, \frac{h(t,\bar{t}) \sin\int_{\bar{t}}^{t}[\varepsilon_a(\tau)-\varepsilon_F]d\tau - \sin\{[\varepsilon_a(t)-\varepsilon_F](t-\bar{t})\}}{\beta \sinh\frac{\pi(t-\bar{t})}{\beta}} \ , \end{aligned} \tag{3.13}$$

where the function $h(t,\bar{t})$ is given by

$$h(t,\bar{t}) = \sqrt{\frac{\Gamma(\bar{t})}{\Gamma(t)}} \exp\left(-\int_{\bar{t}}^{t} d\tau \frac{\Gamma(\tau)}{2}\right) \ . \tag{3.14}$$

Equations (3.12), (3.13), and (3.14) provide an exact solution to the single-level problem.

The validity of the SCA depends on the magnitude of $c(t)$. In Appendix B, we show that the SCA applies in the low-velocity and high-temperature limit.

In order to test the accuracy of the SCA with specific examples we have to specify motion of the atom and its energy levels outside the surface. In the following, we will assume linear motion of the atom. The atom is assumed to start at a distance $Z_1 = 20$ a.u., and to move with constant speed v to the turning point at $Z_2 = 5$ a.u. The atom then reverses direction and moves toward the vacuum, again with constant speed v. At $Z_3 = 20$ a.u. the trajectory is completed. The energy levels of the atom are assumed to shift linearly with distance so that

$$\varepsilon_a(t) = \varepsilon_F + b[Z(t) - Z_c] \ . \tag{3.15}$$

The atomic level thus crosses the Fermi energy at a distance $Z = Z_c$. The width of the energy level is assumed to vary exponentially, i.e.,

$$\Gamma(t) = \Delta \exp[-\alpha Z(t)] \ . \tag{3.16}$$

These assumptions qualitatively describe how atomic affinity levels shift outside a perfect metal or how neutral energy levels would shift outside an alkali-promoted metal surface.[2] The conclusions in this paper are not dependent on the details of these assumptions.

In Fig. 2 we plot the result from the SCA for different velocities. To facilitate the comparison, the tunneling matrix elements have been scaled with velocity so that similar charge transfer will occur for each trajectory. It can be seen that the master equation well describes the charge-transfer dynamics for all velocities considered. Even for large velocities, where the correction $c(z)$ can be very large, the oscillatory behavior of $c(z)$ with distance z tends to cancel the effects of the correction. For low velocities, the corrections are small for all times and the master equation well describes the instantaneous population of the level.

In Fig. 3, $n_a(z)$ is plotted as a function of t for different temperatures. It can clearly be seen that the magnitude of $c(z)$ decreases with temperature.

B. Large-U limit

Using the previously defined notation, the Dyson equation for $G_\sigma^{<}$ takes the form

$$i\frac{\partial}{\partial t}\tilde{G}^{<}_{\sigma}(t,t') = \int_{-\infty}^{\infty} d\bar{t}\,\sqrt{\Gamma_\sigma(t)\Gamma_\sigma(\bar{t})}\,\tilde{f}^{>}_{\sigma}(t,\bar{t})B^{R}(t,\bar{t})\tilde{G}^{<}_{\sigma}(\bar{t},t') + \int_{-\infty}^{\infty} d\bar{t}\,\sqrt{\Gamma_\sigma(t)\Gamma_\sigma(\bar{t})}\,\tilde{f}^{<}_{\sigma}(t,\bar{t})B^{<}(t,\bar{t})\tilde{G}^{A}_{\sigma}(\bar{t},t') \ . \tag{3.17}$$

Assuming that all rapid oscillation with respect to $\bar{t}$ is contained in the functions $\tilde{f}^{\gtrless}$, the SCA leads to

$$\frac{d}{dt}n_\sigma(t) = -\Gamma_\sigma(t)\left[f^{>}(\varepsilon_\sigma(t))n_\sigma(t) - f^{<}(\varepsilon_\sigma(t))n_B(t)\right] \ . \tag{3.18}$$

One could derive a similar sort of equation for $n_B(t)$, but this is unnecessary since our approximations preserve the exact conservation of Q_B, so that $n_B(t)$ is determined simply by

$$n_B(t) = 1 - \sum_\sigma n_\sigma(t). \tag{3.19}$$

The master equation (3.18) coupled with (3.19) therefore determine the semiclassical (SCA) solution.

In order to make (3.18) more intuitive, we give a simple golden rule derivation of it. We note that Γ is the conditional probability per unit time for an electron to tunnel from the atomic state into a band state in the solid with the emission of a boson, given that there was initially an electron in the atomic state, none in the band state, and no bosons present. The nonconditional rate at which the atomic state is emptied is therefore $\Gamma_\sigma(1-f_\sigma)(n_B+1)n_\sigma$, where we have suppressed the time arguments, and abbreviated $f^{<}(\varepsilon_\sigma)$ by f_σ. Similarly the rate at which the atomic state is filled is $\Gamma_\sigma f(\varepsilon_\sigma)n_B(1-n_\sigma)$. Thus the net filling rate is

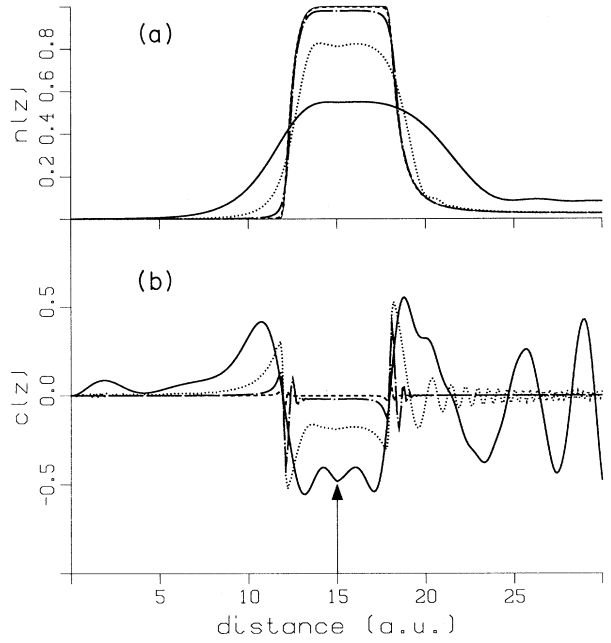

FIG. 2. Effects of velocity on the validity of the SCA for a one-level system ($U = 0$). The motion of the atom is linear and the atomic trajectory is assumed to start towards the surface at $Z = 20$ a.u., to turn towards vacuum at $Z = 5$ a.u., and then to propagate back to $Z = 20$ a.u. The turning point is indicated with an arrow on the horizontal axis. The upper part of the figure shows the occupation $n(z)$ as a function of distance traveled, calculated using Eq. (3.12). The lower part of the figure shows the correction term $c(z)$. The parameters of the system are $Z_c = 8$ a.u., $b = 0.02$, and $\alpha = 0.5$. The temperature is $T = 300$ K and the Fermi energy is 0.2 a.u. The widths of the impurity level have been scaled for each velocity so that similar charge transfer occurs within each trajectory. The solid curves are for $v = 0.1000, \Delta = 10.0$, the dotted curves are for $v = 0.0100, \Delta = 1.0$, the chain-dotted curves are for $v = 0.0010, \Delta = 0.1$ and the dashed lines are for $v = 0.0001, \Delta = 0.01$. For comparison, the result from the master equation, Eq. (3.8), is shown with the thin solid line.

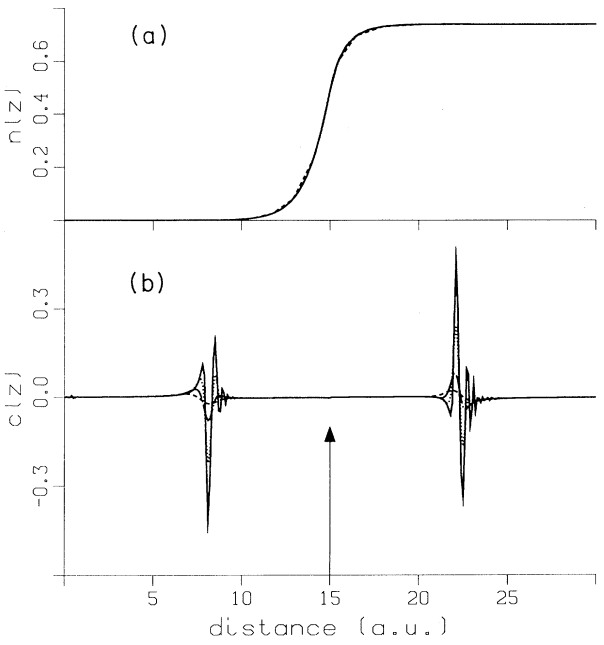

FIG. 3. Effects of temperature on the validity of the SCA for a one-level system ($U = 0$). The trajectory is as in Fig. 2. $Z_c = 12$ a.u., $b = 0.02$, $\Delta = 0.1$ a.u., and $\alpha = 1.0$. The velocity is $v = 0.001$ and the work function is 0.2 a.u. The upper part of the figure shows the occupation $n(z)$ as function of distance traveled, calculated using Eq. (3.12). The lower part of the figure shows the correction term $c(z)$. The solid curves are for $T = 300$ K, the dotted curves are for $T = 600$ K, the dash-dotted curves are for $T = 1200$ K, and the dashed lines are for $T = 2400$ K.

$$\frac{dn_\sigma}{dt} = \Gamma_\sigma f_\sigma n_B(1-n_\sigma) - \Gamma(1-f_\sigma)(n_B+1)n_\sigma . \tag{3.20}$$

The above equation disagrees with (3.18) because we have not yet made the projections onto the $Q_B = 1$ subset of states. This is done as before by omitting terms that are quadratic or higher in Q_B. Noting that both n_σ and n_B are each first order in Q_B, we obtain

$$\frac{dn_\sigma}{dt} = \Gamma_\sigma f_\sigma \left(1 - \sum_\sigma n_\sigma\right) - \Gamma_\sigma(1-f_\sigma)n_\sigma , \tag{3.21}$$

where we have used (3.19) to eliminate n_B after making the projections indicated above. The meaning of (3.21) becomes clearly apparent if we write the $U = 0$ master equation (3.8) in a similar form:

$$\frac{dn_\sigma}{dt} = \Gamma_\sigma f_\sigma (1-n_\sigma) - \Gamma_\sigma(1-f_\sigma)n_\sigma . \tag{3.22}$$

The only difference between the two equations is that the Pauli exclusion factor $(1-n_\sigma)$ in the $U = 0$ case has been replaced by the much stronger Coulomb exclusion factor $(1-\sum_\sigma n_\sigma)$ in the $U = \infty$ case.

The difference between the instantaneous equilibrium values of n_σ toward which each type of master equation drives can also be understood simply. Equation (3.22) clearly relaxes toward $n_\sigma = f_\sigma$, that is to the Fermi-Dirac distribution, which is appropriate for noninteracting fermions correlated only by statistics. On the other hand, Eq. (3.21) relaxes toward a more complicated distribution given by the solution of the equations

$$n_\sigma = \frac{f_\sigma}{1-f_\sigma}\left(1 - \sum_\sigma n_\sigma\right) . \tag{3.23}$$

These equations are not immediately transparent, but are in fact the equations that determine the equilibrium occupations of a multiple state $U = \infty$ Anderson model with $V = 0$. For a two-state model ($\sigma = \pm 1$), one obtains

$$n_\sigma = f_\sigma(1-f_{-\sigma})/(1-f_\sigma f_{-\sigma}) . \tag{3.24}$$

This gives $n_\sigma = \frac{1}{2}$ for a degenerate level way below the Fermi level. This is expected because it corresponds to a total occupation $n_\sigma + n_{-\sigma} = 1$.

It should also be clear at this point that it is not necessary to make the approximation of separable time dependence of V, nor of constant $V^2\rho$, if we are also going to make the SCA. In these master equations, we simply take

$$\Gamma_\sigma(t) = 2\pi \left|V_{\varepsilon_\sigma(t)}(t)\right|^2 \rho(\varepsilon_\sigma(t)) \tag{3.25}$$

within the Anderson model. More generally $\Gamma_\sigma(t)$ is the adiabatic one-electron width of the atomic level with the atom frozen in the position in which it would be at time t. An accurate method for calculating these widths has recently been proposed.[20]

In the large-U limit we can immediately see that the requirements on the SCA will be much more stringent than in the $U = 0$ situation. First it must be required that the atomic levels cross the Fermi energy rapidly. In addition, since the charge transfer will depend on the instantaneous occupancy of the various levels, we must require that the master equation accurately represent the population of the respective levels for all t.

We now derive an improved master equation for $U = \infty$ analogous to Eq. (3.12) for $U = 0$. We follow a procedure similar to that used for the $U=0$ situation, although here it is no longer exact, as explained below. However, by comparing our improved treatment with the results of the SCA, we obtain a clear indication of the size of the errors to be expected in the latter.

The improvement which is made over the SCA solution to Eq. (3.17) is to use approximate forms for $B^R(t,\bar{t})$ and $\tilde{G}^A_\sigma(\bar{t},t')$ for unequal time arguments, rather than to approximate them by their equal time values. Approximate expressions for these Green's functions can be derived by applying the SCA to their corresponding Dyson equations. For the $U = 0$ case, the SCA for the retarded and advanced Green's functions was exact, and because of the absence of the slave-boson propagator and the time locality of $\Sigma^{R,A}$, no more approximation was necessary. The use of an approximate form for the retarded and advanced Green's functions combined with the SCA limit the possibilities for the accurate description of the fluctuations leading to the highly correlated mixed-valent state or the Kondo state. Such effects are, however, not thought to be important for the atomic scattering problem under consideration here.

Applying the SCA to Eq. (3.17) we obtain

$$i\frac{\partial}{\partial t}\tilde{G}^<_\sigma(t,t') = \int_{-\infty}^{\infty} d\bar{t}\,\sqrt{\Gamma_\sigma(t)\Gamma_\sigma(\bar{t})}\,\tilde{f}^>_\sigma(t,\bar{t})B^R(t,\bar{t})\tilde{G}^<_\sigma(t,t') + \int_{-\infty}^{\infty} d\bar{t}\,\sqrt{\Gamma_\sigma(t)\Gamma_\sigma(\bar{t})}\,\tilde{f}^<_\sigma(t,\bar{t})B^<(t,t)\tilde{G}^A_\sigma(\bar{t},t') . \tag{3.26}$$

The Dyson equation for the retarded Green's functions have the form

$$\begin{aligned} i\frac{\partial}{\partial t}\tilde{G}^R_\sigma(t,t') &= \delta(t-t') + \int_{-\infty}^{\infty} d\bar{t}\,\sqrt{\Gamma_\sigma(t)\Gamma_\sigma(\bar{t})}\,\tilde{f}^>_\sigma(t,\bar{t})B^R(t,\bar{t})\tilde{G}^R_\sigma(\bar{t},t') , \\ i\frac{\partial}{\partial t}B^R(t,t') &= \delta(t-t') + \sum_\sigma \int_{-\infty}^{\infty} d\bar{t}\,\sqrt{\Gamma_\sigma(t)\Gamma_\sigma(\bar{t})}\,\tilde{f}^<_\sigma(\bar{t},t)\tilde{G}^R_\sigma(t,\bar{t})B^R(\bar{t},t') . \end{aligned} \tag{3.27}$$

In these expressions, the imaginary part of $\tilde{f}^{\gtrless}(t,t')$ will also contribute. This will result in a shift of the bare

impurity levels. The imaginary part of $\tilde{f}^{\gtrless}(t,t')$ is strongly peaked at $t=t'$ (in the infinite band limit, $\mathrm{Im}\tilde{f}$ diverges as $[\sinh\pi(t-t')/\beta]^{-1}$ and for the finite band the imaginary part will be localized within a time interval $\delta t = 1/D$). The SCA can thus still be performed and in Appendix C it is shown that the following approximate expressions for the retarded Green's functions are obtained:

$$\tilde{G}^R_\sigma(t,t') = -i\Theta(t-t')\exp\left(-\int_{t'}^{t} d\tau\,\frac{\Gamma_\sigma(\tau)}{2} f^{>}(\varepsilon_\sigma(\tau))\right) ,$$
$$B^R(t,t') = -i\Theta(t-t')\exp\left(-\int_{t'}^{t} d\tau\,\sum_\sigma \frac{\Gamma_\sigma(\tau)}{2} f^{<}(\varepsilon_\sigma(\tau))\right) . \tag{3.28}$$

To get an estimate of the error that is introduced in the SCA, these expressions can be inserted in Eq. (3.26), and one finds that

$$\frac{\partial}{\partial t}\tilde{G}^{<}_\sigma(t,t') = -\tilde{G}^{<}_\sigma(t,t')\int_{-\infty}^{t} d\bar{t}\,\sqrt{\Gamma_\sigma(t)\Gamma_\sigma(\bar{t})}\,\tilde{f}^{>}_\sigma(t,\bar{t})\exp\left(-\int_{\bar{t}}^{t} d\tau\,\sum_\sigma\frac{\Gamma_\sigma(\tau)}{2} f^{<}(\varepsilon_\sigma(\tau))\right)$$
$$+ B^{<}(t,t)\int_{-\infty}^{t'} d\bar{t}\,\sqrt{\Gamma_\sigma(t)\Gamma_\sigma(\bar{t})}\,\tilde{f}^{<}_\sigma(t,\bar{t})\exp\left(\int_{t'}^{\bar{t}} d\tau\,\frac{\Gamma_\sigma(\tau)}{2} f^{>}(\varepsilon_\sigma(\tau))\right) . \tag{3.29}$$

These equations can be rewritten in terms of functions $d^{\gtrless}_\sigma(t)$ so that the master equation takes the form

$$\frac{d}{dt}n_\sigma(t) = -\Gamma_\sigma(t)n_\sigma(t)[f^{>}(\varepsilon_\sigma(t)) + d^{<}_\sigma(t)] + \Gamma_\sigma(t)n_B(t)[f^{<}(\varepsilon_\sigma(t)) - d^{>}_\sigma(t)] . \tag{3.30}$$

The functions $d^{\gtrless}_\sigma(t)$ have the form

$$d^{\gtrless}_\sigma(t) = \int_{-\infty}^{t} d\bar{t}\,\frac{\delta^{\gtrless}_\sigma(t,\bar{t})\sin\int_{\bar{t}}^{t}[\varepsilon_\sigma(\tau)-\varepsilon_F]d\tau - \sin\{[\varepsilon_\sigma(t)-\varepsilon_F](t-\bar{t})\}}{\beta\sinh\frac{\pi(t-\bar{t})}{\beta}} , \tag{3.31}$$

where

$$\delta^{>}_\sigma(t,t') = \sqrt{\frac{\Gamma_\sigma(t')}{\Gamma_\sigma(t)}}\exp\left(-\int_{t'}^{t} d\tau\,\frac{\Gamma_\sigma(\tau)}{2} f^{>}(\varepsilon_\sigma(\tau))\right) , \tag{3.32}$$

and

$$\delta^{<}_\sigma(t,t') = \sqrt{\frac{\Gamma_\sigma(t')}{\Gamma_\sigma(t)}}\exp\left(-\int_{t'}^{t} d\tau\,\sum_\sigma\frac{\Gamma_\sigma(\tau)}{2} f^{<}(\varepsilon_\sigma(\tau))\right). \tag{3.33}$$

Note that Eq. (3.19) is valid here as well. Therefore Eqs. (3.30) and (3.19) form a closed set of equations, when coupled with the definitions (3.31), (3.32), and (3.33). It is a straightforward matter to solve them numerically for given $\varepsilon_\sigma(t)$ and $\Gamma_\sigma(t)$.

We note also that Eq. (3.30) reduces to the master equation, Eq. (3.18), when the functions $d^{\gtrless}_\sigma$ are small. The functions $d^{\gtrless}(t)$ are similar to the function $c(t)$ defined for the $U=0$ case. In Appendix B, it is shown that these functions also vanish in the low-velocity and high-temperature limit. A simple case in which it is possible to demonstrate that our approximation represents an improvement over the SCA is for the situation with two slowly varying levels, one well above and the other well below the Fermi level. By this we mean $\Gamma_\sigma/|\varepsilon_\sigma-\varepsilon_F| \ll 1$ and $\exp(-\beta|\varepsilon_\sigma-\varepsilon_F|) \ll 1$. The equilibrium occupation numbers can be obtained by setting the left side of (3.30) equal to zero and solving the coupled equations for the occupation numbers. When $\Gamma\beta/2\pi \ll 1$ [the condition (B9) for the validity of the SCA at $v=0$], one obtains a result agreeing with the appropriate limit of the semiclassical result (3.24). On the other hand, in the opposite limit $\Gamma\beta/2\pi \gg 1$, one obtains for the occupation of the level below the Fermi level

$$n_1 = 1 - \Gamma_1/2\pi(\varepsilon_F - \varepsilon_1), \tag{3.34}$$

while the occupation of the level above the Fermi level remains negligibly different from zero. Both these results agree with what can be trivially derived by second-order zero-temperature perturbation theory, which obviously applies exactly in the limit considered here. Thus our procedure gives the correct result in this case, even though the criterion (B9) for the SCA is not satisfied, and when the SCA does not give the right value. We should mention, however, that for both levels below the Fermi level, the criterion (B9) still must be satisfied for our equations to give the correct result. This is not unexpected since the approximate forms for the advanced and retarded Green's functions derived in Appendix C require that $\Gamma\beta/2\pi$ be small.

In order to test the SCA for the infinite-U model, we introduce two atomic energy levels, $|1\rangle$ and $|2\rangle$, as above. The dependences of the shift and broadening of these levels with distance are again assumed to be linear and exponential, respectively, following Eqs. (3.15) and (3.16). We assume that the atom moves with constant speed

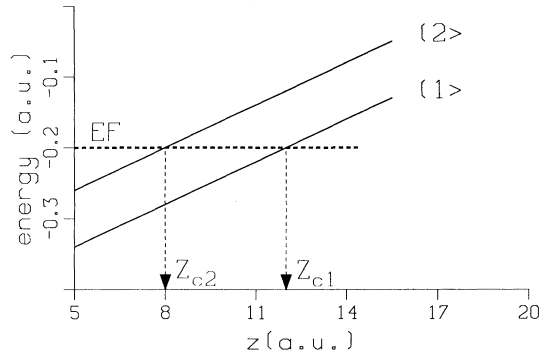

FIG. 4. Schematic plot of the assumed shift of the two atomic energy levels $|1\rangle$ and $|2\rangle$ near a metal surface. The Fermi energy and the crossing distances Z_c^1 and Z_c^2 where the atomic energy level crosses the Fermi energy are indicated.

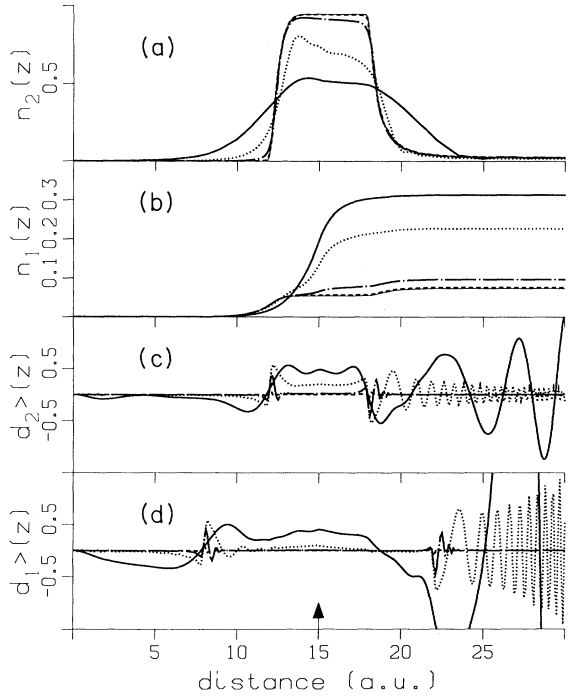

FIG. 5. Effects of the velocity on the validity of the master equation for two levels in the infinite-U limit. The two top figures (a) and (b) show the populations $n_2(z)$ and $n_1(z)$ calculated using Eq. (3.30), as a function of distance traveled. (c) shows the magnitude of the correction term $d^>(z)$ for level 2. In (d), the correction term $d^>(z)$ for level 1 is shown. The calculations are performed assuming two levels with $Z_c^1 = 12$ a.u., $Z_c^2 = 8$ a.u., $b_1 = b_2 = 0.02$, $\alpha_1 = 1.0$, $\alpha_2 = 0.5$, $T = 300$ K and the metal work function is 0.2 a.u. The widths have been scaled so that similar charge transfer occurs during each trajectory. The solid curves are for $v = 0.1000$, $\Delta_{1,2} = 10.0$, the dotted curves are for $v = 0.0100$, $\Delta_{1,2} = 1.0$, the dash-dotted curve is for $v = 0.0010$, $\Delta_{1,2} = 0.1$, and the dashed lines are for $v = 0.0001$, $\Delta_{1,2} = 0.01$. The populations $n_1(z)$ and $n_2(z)$ obtained using Eq. (3.18) neglecting the correction terms $d^{\gtrless}$ are shown with the thin solid line in (b) and (a), respectively.

v following the straight-in—straight-out trajectory described earlier. In Fig. 4, the shift of the atomic levels as a function of distance from the surface is schematically illustrated and the respective crossing distances Z_c^1 and Z_c^2 and the Fermi energy indicated.

In Fig. 5, the populations $n_1(z)$ and $n_2(z)$ are shown as a function of distance for different velocities. In the lower part of the figure, the variation of $d_1^>$ and $d_2^>$ is shown as a function of distance from the surface. It can clearly be seen that the functions $d(z)$ vanish with decreasing velocity. In Fig. 6, trajectories are shown for different substrate temperature. Analogous to the $U = 0$ situation, the corrections $d_1^<$ and $d_2^<$ decrease with increasing temperature. As will be evident in the result section, the requirements for the SCA to apply are more stringent than in the $U = 0$ situation. Since the charge-transfer dynamics in the presence of intra-atomic correlation will depend on the instantaneous population of all atomic energy levels in the problem, it is crucial that the instantaneous populations of all energy levels are accurately described. This can directly be seen in Fig. 5, where an accurate population of level $|1\rangle$ only is obtained at room temperature.

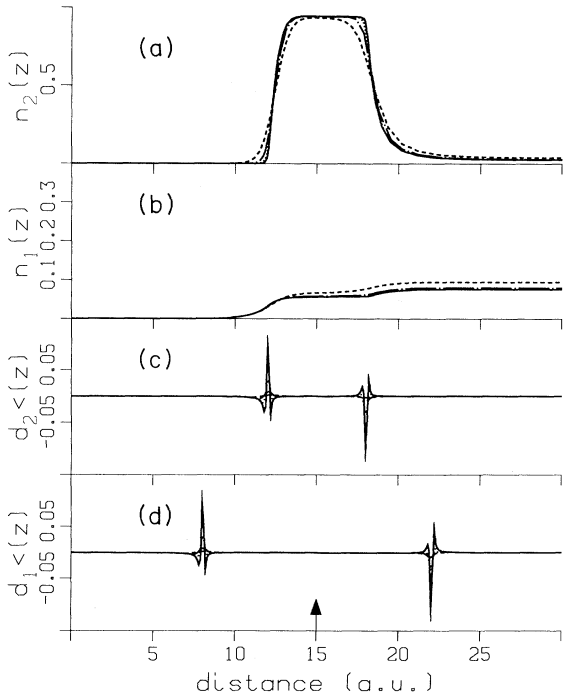

FIG. 6. Effects of temperature on the validity of the master equation for two levels in the infinite-U limit. The trajectory and energy level parameters are taken as in Fig. 4. The velocity is $v = 0.001$ and the Fermi energy is 0.2 a.u. The top figures (a) and (b) show the populations $n_2(z)$ and $n_1(z)$ as obtained using Eq. (3.30). (c) shows the correction term $d_2^<(z)$. (d) shows the correction term $d_1^<(z)$. The solid curves are for $T = 300$ K, the dotted curves are for $T = 600$ K, the dash-dotted curves are for $T = 1200$ K, and the dashed lines are for $T = 2400$ K.

IV. APPLICATION TO ION-SURFACE SCATTERING

In the first three subsections we will present some results for charge transfer in atom-surface scattering. The calculations are performed for two levels interacting with the continuum. For simplicity the atomic trajectory and the variation of the shifts and broadening of the atomic levels with distance are taken as described earlier; see (3.15), (3.16), and the corresponding discussion. For comparison we will show both the results obtained using the master equation for infinite U, Eq. (3.18), and the result for each of the levels assuming $U = 0$, Eq. (3.8). It is important to keep in mind that the calculated occupation numbers represent expectation values and thus refer to a macroscopic ensemble of atoms scattered against the surface. In the discussion below, we will, however, refer to individual atomic trajectories. Fractional occupation of the levels should therefore be interpreted as an ensemble average of the occupation. It will be demonstrated that the inclusion of correlation effects can have a drastic effect on the charge-transfer dynamics and lead to qualitatively different results than what a theory neglecting the intra-atomic correlation would predict.

In the last subsection, we will discuss the relevance of our finding of a strong correlation effect on charge transfer for the anomalous yield of positive ions at low velocities in sputtering of metal surfaces.

A. Spin dependent scattering

As was demonstrated in the theory section, the inclusion of spin affects the charge transfer even for the degenerate case. The inclusion of spin can lead to other very important effects that could be probed using spin-polarized atom-surface scattering. In Fig. 7, the scattering of a spin-polarized atom with a surface is modeled. The two spin levels are assumed to be degenerate and the surface is assumed to be nonmagnetic. As the surface is approached, the electron tunnels into the surface and the atom is increasingly ionized. At the position Z_c, where the atomic levels cross the Fermi energy, electrons start to fill the atomic level. At this distance there exists a net spin polarization of the atom. The presence of intra-atomic correlation restricts the occupancy of the atomic levels to one. As the atom moves towards the turning point, the net spin polarization is preserved since the tunneling rates into the different spin levels are the same. Thus even at the turning point close to the surface, an ensemble of atoms would have a net spin polarization. This spin polarizations is naturally maintained also through the outgoing trajectory.

For the $U = 0$ case, both of the spin levels are completely occupied at the turning point due to the very efficient tunneling at such close distances from the surface. All spin polarization is therefore lost and a complete equilibration with the magnetization with the surface results.

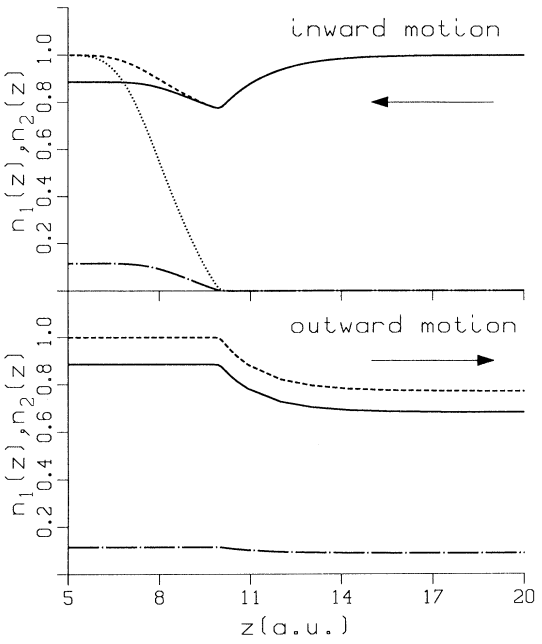

FIG. 7. Comparison of the results from the master equations for infinite U and $U = 0$ for a doubly degenerate atomic level. The trajectory is as defined in Fig. 4. The upper part of the figure shows the population of the different levels as a function of distance from the surface along the ingoing trajectory. The lower figure describes the outgoing trajectory. The parameters of the system are $v = 0.001$, $T = 300$ K, $Z_c^1 = Z_c^2 = 10$ a.u., $b_1 = b_2 = 0.02$, $\Delta_1 = \Delta_2 = 0.2$ a.u., and $\alpha_1 = \alpha_2 = 0.7$ a.u. The metal work function is 0.2 a.u. The solid and dash-dotted lines are $n_1(z)$ and $n_2(z)$ calculated using Eq. (3.18). The dashed and dotted lines are $n_1(z)$ and $n_2(z)$ calculated using Eq. (3.8), i.e., neglecting correlation. During the outgoing trajectory the dotted and dashed lines coalesce, resulting in an apparent dashed line.

B. Multiple levels

In the situation where several levels can be neutralized, the resulting charge state of a desorbing atom will also be determined by dynamical effects. In Fig. 8, we illustrate how the filling of an excited atomic state can prevent the formation of the ground state. The excited state is assumed to cross the Fermi energy closer to the surface than the ground state. The width of the excited state is assumed to be larger and more slowly varying with distance than the width of the ground state.

As the atom approaches the surface it reaches the point where the atomic ground state shifts below the Fermi energy. After this point, the ion can neutralize by resonant tunneling into the ground state. The tunneling rate into this state is, however, low so the probability for neutralization of the ion is very small. At the position where the excited level crosses the Fermi energy, the atom is very efficiently neutralized by resonant tunneling into the excited state. The atom will keep its neutral state through the collision with the surface and during the outgoing

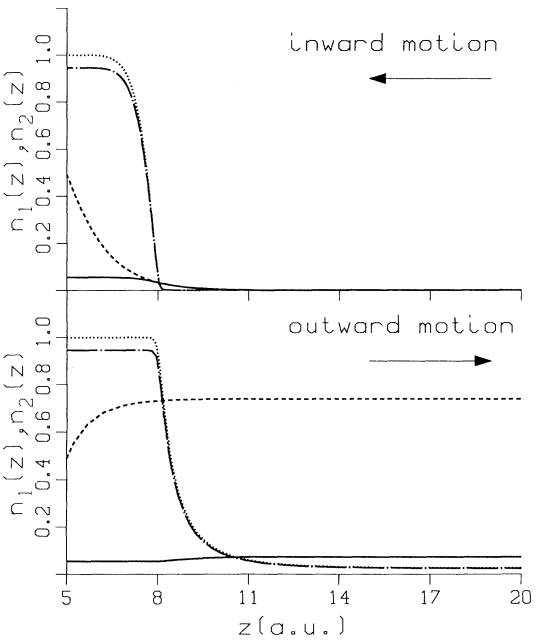

FIG. 8. Comparison between the master equations for infinite U and $U = 0$, for the same levels as described in Figs. 5 and 6. The trajectory and layout of the figure are as described in Fig. 7. The parameters of the system are $v = 0.001$, $T = 300$ K, $Z_c^1 = 12.0$ a.u., $b_1 = b_2 = 0.02$, $\Delta_1 = \Delta_2 = 0.1$, α_1=1.0, $Z_c^2 = 8.0$ a.u., and $\alpha_2 = 0.5$. The work function of the metal is 0.2 a.u. The solid and dash-dotted lines are $n_1(z)$ and $n_2(z)$ calculated using Eq. (3.18). The dashed and dotted lines are $n_1(z)$ and $n_2(z)$ calculated using Eq. (3.8), i.e., neglecting correlation.

trajectory until the excited level crosses the Fermi energy, at which time the excited atom will re-ionize. This ion can now in principle be neutralized by resonant tunneling into the ground state, but since the tunneling rate is low, the reneutralization is inefficient and most of the time the atom will emerge from the surface as an ion.

These results are again in qualitative disagreement with a theory neglecting the intra-atomic correlation. In this case the neutralization of the two levels occurs independently. The ground state will be almost completely filled due to the large tunneling rate into this state close to the surface. As the atom passes the crossing distance and the ground-state level shifts to above the Fermi energy, the atom can re-ionize. However, since the tunneling rate is small at this relatively large distance from the surface, the probability for the atom to emerge as an ion is very low. The neglect of the correlation energy thus wrongly predicts almost complete neutralization of an ensemble of atoms in this scattering experiment.

C. Almost degenerate levels with different widths

In a recent paper[21] it was suggested that the surface-induced hybridization of atomic levels can lead to atomic levels with different geometrical orientation of the atomic wave functions. This effect can result in levels that have almost the same energy while very different widths. Since the energy of these levels is similar, one might expect correlation effects to influence the charge transfer strongly. In Fig. 9, a scattering experiment involving an atom with two almost degenerate levels with different widths is modeled. As the ion passes the crossing distance, the short-lived atomic level gets filled quickly. The occupation of the long-lived atomic level is therefore effectively blocked by the U term. When the atom passes the crossing distance during its outgoing trajectory, the atom starts to re-ionize. Since the tunneling rate into the long-lived state is zero this state can no longer be formed and the probability for the atom to emerge neutralized is vanishingly small.

The neglect of intra-atomic correlation in this situation again would yield a qualitatively different result for an ensemble of atoms scattered against the surface. As the levels approach the surface they will be filled independently of each other and at the turning point, both levels are occupied. When the atoms have passed the crossing

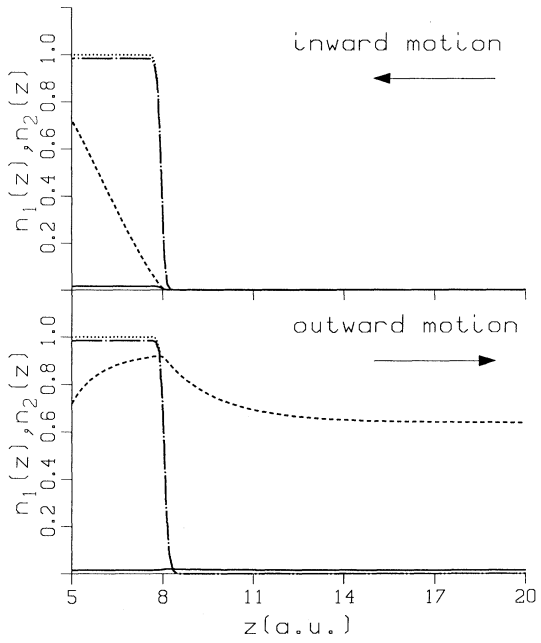

FIG. 9. Comparison between the master equations for infinite U and $U = 0$, for two degenerate resonances with very different widths. The trajectory and layout of the figure are as described in Fig. 7 The parameters of the system are $v = 0.001$, $T = 300$ K, $Z_c^1 = Z_c^2 = 8.0$ a.u., $b_1 = b_2 = 0.02$, $\Delta_1 = 0.01$, $\Delta_2 = 1.0$, and $\alpha_1 = \alpha_2 = 1.0$. The work function of the metal is 0.2 a.u. The solid and dash-dotted lines are $n_1(z)$ and $n_2(z)$ calculated using Eq. (3.18). The dashed and dotted lines are $n_1(z)$ and $n_2(z)$ calculated using Eq. (3.8), i.e., neglecting correlation. During the outgoing trajectory, the dotted and dash-dotted lines coalesce, resulting in an apparent dash-dotted line.

point, the atoms in the short-lived state immediately reionize. The atoms in the long-lived state do, however, survive. This conclusion is entirely different from that for the infinite-U model.

D. Application to sputtering experiments

In several recent sputtering experiments an increase in the yield of positive ions emerging from the surface at low velocities has been observed,[22] compared to what would be expected from interpretations neglecting correlation effects.

Attempts to explain these anomalous results in terms of intra-atomic correlation effects have been only partly successful.[11] These authors found that for the spin-dependent case, one could expect a reduction in the neutralization rates of the level below the Fermi energy due to correlation. The proposed effect was judged too small to account for the experimental results. In light of the present theory, where it has been demonstrated how excited atomic states can prevent the formation of certain more equilibrated states, the presence of intra-atomic correlation could possibly have a larger effect than that which was proposed by Brako and Newns.[11] Thus temporary excited atomic states might be formed close to the surface that would prevent the formation of the ground state. As the excited atom leaves the surface region, it will ionize.

In view of the strong perturbations expected on the surface electronic structure in sputtering, a detailed comparison between experiments and theory is, however, not possible.

V. CONCLUSIONS

We have presented a convenient method for describing charge-transfer processes in atom-surface collisions. The method is based on the double-time Green's-function method developed by Kadanoff and Baym to treat nonequilibrium phenomena. Using the slave-boson method, a solution of the time-dependent Anderson model for infinite U can be given in terms of a coupled set of integral equations. We have shown that under certain conditions, such as high temperature and low velocities, the general equations simplify and a set of coupled master equations for the charge transfer results. This finding is of considerable importance since it allows the description of charge transfer on the same level as the description of the nuclear motion. Applications of this master equation to a number of different atom-surface-scattering situations have shown that the inclusion of intra-atomic correlation can have a profound effects on the charge-transfer processes that can occur. In the cases presented, the inclusion of correlation gives a qualitatively different behavior than what would have been expected for a single-level situation. Even the inclusion of spin for a single level can lead to a qualitatively different result from the spinless approximation. The method and solution presented are expected to apply to a wide class of nonequilibrium phenomena involving time-dependent perturbations and intra-atomic correlation effects.

ACKNOWLEDGMENTS

Acknowledgment is made to the Donors of The Petroleum Research Fund, administered by the American Chemical Society, for the partial support of this research. This work is supported in part by the National Science Foundation under Grant No. DMR-88-01027.

APPENDIX A: SOME USEFUL IDENTITIES

In this appendix some of the identities used in the text are listed. These were all previously derived for fermions.[16] Here we need to consider bosons as well as combinations of bosons and fermions.

First we give some definitions. Let $C(t,t')$ be a propagatorlike object, either fermionlike or bosonlike. Examples of "propagatorlike objects" would be propagators (Green's functions) and self-energies. The analytic pieces of C, that is $C^>$ and $C^<$, are defined by

$$iC(t,t') = C^>(t,t')\Theta(t-t') \pm C^<(t,t')\Theta(t'-t) , \tag{A1}$$

where $\Theta(t-t')$ is a unit step function that operates along the (possibly complex) integration contour, and where the upper sign is to be used for bosons and the lower sign for fermions. This sign convention holds throughout this appendix, *but not elsewhere*. Similarly we define the advanced and retarded functions by

$$\begin{aligned} iC^R(t,t') &= \Theta(t-t')[C^>(t,t') \mp C^<(t,t')], \\ iC^A(t,t') &= -\Theta(t'-t)[C^>(t,t') \mp C^<(t,t')] . \end{aligned} \tag{A2}$$

Suppose C is given by a *series product* of A and B:

$$C(t,t') = \int_c dt''\, A(t,t'')B(t'',t') , \tag{A3}$$

where c is the appropriate complex contour. For example, the integrals involving the self-energy times the Green's function in the Dyson equation are of this type. Note that if C is fermionlike, so are A and B; if C is bosonlike then so also are A and B. The key identities that enable one to continue integrals like this to the real axis are

$$\begin{aligned} C^{\gtrless}(t,t') = \int_{-\infty}^{\infty} dt''\, [\, & A^R(t,t'')B^{\gtrless}(t'',t') \\ & + A^{\gtrless}(t,t'')B^A(t'',t')] , \end{aligned} \tag{A4}$$

and

$$C^{R,A}(t,t') = \int_{-\infty}^{\infty} dt''\, A^{R,A}(t,t'')B^{R,A}(t'',t'). \tag{A5}$$

These hold both for bosonlike and fermionlike objects.

Suppose on the other hand C is given by a *parallel*

product of B and C. It is trivial here to continue to the real axis, but is is still useful to express the results in terms of the advanced, retarded, greater-than, and lesser-than quantities. There are two cases of interest, one where C is bosonlike, which means that A and B represent a fermion—antifermion pair as in the self-energy of the slave boson, a second where C is fermionlike, which means that A and B, respectively, represent a fermion and a boson as in the self-energy of the atomic levels. In the first case we define

$$C(t,t') = A(t,t')B(t',t) \ . \tag{A6}$$

Use of the definitions above gives

$$C^{\gtrless}(t,t') = iA^{\gtrless}(t,t')B^{\lessgtr}(t',t) \tag{A7}$$

and

$$C^{R,A}(t,t') = i[\ A^{>}(t,t')B^{R,A}(t',t) - A^{R,A}(t,t')B^{>}(t',t)] \ . \tag{A8}$$

Similarly in the second case we define

$$C(t,t') = A(t,t')B(t,t'). \tag{A9}$$

Assuming that A is fermionlike and B is bosonlike, we obtain

$$C^{\gtrless}(t,t') = -iA^{\gtrless}(t,t')B^{\gtrless}(t,t') \tag{A10}$$

and

$$C^{R,A}(t,t') = -i[\ A^{>}(t,t')B^{R,A}(t,t') A^{R,A}(t,t')B^{<}(t,t')] \ . \tag{A11}$$

The above identities were used a number of times in the development in the main text, without specific reference to this appendix.

APPENDIX B: VALIDITY OF THE SEMICLASSICAL APPROXIMATION

In this appendix we will discuss the validity of the SCA. The quality of the SCA will depend on the magnitude of the corrections terms $c(t)$ and $d^{\gtrless}(t)$. The SCA involves an approximation of the following form:

$$\int_{-\infty}^{t} d\bar{t}\ \sqrt{\Gamma(t)\Gamma(\bar{t})}\,\mathrm{Re}[\tilde{f}^{\gtrless}(t,\bar{t})]\tilde{G}^{A}(\bar{t},t) \approx \tilde{G}^{A}(t,t)\Gamma(t)\int_{-\infty}^{t} d\bar{t}\,\mathrm{Re}[\tilde{f}^{\gtrless}(t,\bar{t})] \ , \tag{B1}$$

where

$$\mathrm{Re}[\tilde{f}^{\gtrless}(t,\bar{t})] = \tfrac{1}{2}\delta(t-\bar{t}) \pm \frac{1}{2}\frac{\sin\int_{\bar{t}}^{t} d\tau[\varepsilon_a(\tau)-\varepsilon_F]}{\beta\sinh\frac{\pi(t-\bar{t})}{\beta}} \ , \tag{B2}$$

where the plus sign goes with $f^{>}$ and the minus with $f^{<}$.

We note that there are two independent factors that will contribute to the localization in $\bar{t}$. The denominator involves a hyperbolic sine term that will cut off contributions where $t-\bar{t} > \beta/\pi$. This defines a time interval Δt_1 during which the integrand in Eq. (B1) must be stationary. The oscillatory nature of the sine term in the denominator restricts the time integration to a time interval, $t-\bar{t} < [\varepsilon_F - \varepsilon_a(t)]^{-1}$. This defines another time interval Δt_2 during which the integrand in Eq. (B1) must vary slowly. The latter cutoff will be in effect as long as the atomic level is far from the Fermi energy.

The variation of the integrand in Eq. (B1) should be small during the smallest of these time intervals. Assuming exponential level widths and uniform velocity as discussed in the theory section, Γ varies with time as $\exp(-\alpha v t)$. For the $U=0$ case, G^A has the following form:

$$G^{A}(t,\bar{t}) = \exp\left(\int_{t-\bar{t}}^{t} d\tau\,\frac{\Gamma(\tau)}{2}\right) \ , \tag{B3}$$

and for the correlated system, G_A is of either the form

$$G^{A}(t,\bar{t}) = \exp\left(\int_{t-\bar{t}}^{t} d\tau\,\frac{\Gamma(\tau)}{2} f^{>}(\varepsilon_\sigma(\tau))\right) \tag{B4}$$

or

$$G^{A}(t,\bar{t}) = \exp\left(\int_{t-\bar{t}}^{t} d\tau\,\sum_{\sigma}\frac{\Gamma(\tau)}{2} f^{<}(\varepsilon_\sigma(\tau))\right) \ . \tag{B5}$$

All of these functions G^A are similar so in the following we will use the last form. For small times $\bar{t}$, G^A varies with time as

$$G^{A}(t,\bar{t}) \approx \exp\left(\sum_{\sigma}\Gamma_\sigma(t)\frac{(t-\bar{t})}{2} f^{<}(\varepsilon_\sigma(t))\right) \ . \tag{B6}$$

The conditions for the SCA are thus that the variation of

$$\exp\left(\frac{\alpha v}{2}(t-\bar{t}) - \sum_{\sigma}\frac{\Gamma_\sigma(t)}{2} f^{<}(\varepsilon_\sigma)(t-\bar{t})\right) \tag{B7}$$

is slow during the smallest of the time intervals Δt_1 or Δt_2. Using $\Delta t_1 = \beta/\pi$, we obtain the following criterion:

$$\left|\alpha v - \sum_{\sigma}\Gamma_\sigma(t)\right|\frac{\beta}{2\pi} \ll 1. \tag{B8}$$

This condition is satisfied at high temperatures and low velocities, and leads to the following conditions:

$$\sum_{\sigma}\Gamma_\sigma(t) \ll \frac{2\pi}{\beta} \qquad \alpha v \ll \frac{2\pi}{\beta} \ . \tag{B9}$$

The alternative condition for the SCA due to the possible smallness of Δt_2 leads to the condition

$$\left|\frac{\alpha v - \sum_{\sigma}\Gamma_\sigma(t)}{\varepsilon_a(t)-\varepsilon_F}\right| \ll 1 \ . \tag{B10}$$

In practical applications, the αv term will be much smaller than the term involving the widths Γ and can therefore be neglected. The criterion thus takes the form:

$$\frac{\sum_\sigma \Gamma_\sigma(t)}{|\varepsilon_a(t)-\varepsilon_F|} \ll 1 . \tag{B11}$$

Obviously this criterion does not apply at times where the atomic energy levels cross the Fermi energy. This is, however, often the situation of relevance for experiments. For the SCA to apply in the low-temperature limit we must therefore require that only very small charge transfer occur during the time of crossing of an atomic energy level with the Fermi energy. The crossing time Δt_c can be directly obtained from Eq. (B10), $\Delta t_c = \sum_\sigma(\Gamma_\sigma/bv)$, where

$$b = \frac{d}{dz}\varepsilon_a(z)\bigg|_{z=z_c} . \tag{B12}$$

The charge transfer during this time is proportional to $\Gamma_\sigma(t_c)$. The condition of small charge transfer during the crossing translates into the following requirement on the velocity:

$$v > \Gamma^2(Z_c)\left(\frac{d}{dz}\varepsilon_a(Z_c)\right)^{-1} . \tag{B13}$$

We now turn to the evaluation of the remaining integral in Eq. (B1),

$$\int_{-\infty}^{t} d\bar{t}\,\mathrm{Re}[\tilde{f}^{\gtrless}(t,\bar{t})]$$

$$= \tfrac{1}{4} \pm \tfrac{1}{2}\int_{-\infty}^{t} d\bar{t}\,\frac{\sin\int_{\bar{t}}^{t} d\tau\,[\varepsilon_a(\tau)-\varepsilon_F]}{\beta\sinh\frac{\pi(t-\bar{t})}{\beta}} . \tag{B14}$$

To facilitate the discussion, the function $\Lambda(t,\bar{t})$ is defined as

$$\Lambda(t,\bar{t}) = \int_{\bar{t}}^{t} d\tau[\varepsilon_a(\tau)-\varepsilon_F] . \tag{B15}$$

For $\varepsilon_a(t)$ constant in time, Λ takes a simple form:

$$\Lambda(t,\bar{t}) = (\varepsilon_a-\varepsilon_F)(t-\bar{t}) . \tag{B16}$$

The integration in Eq. (B14) can here trivially be performed and gives

$$\int_{-\infty}^{t} d\bar{t}\,\mathrm{Re}[\tilde{f}^{\gtrless}(t,\bar{t})] = \tfrac{1}{4} \pm \tfrac{1}{2}[\tfrac{1}{2} - f^{<}(\varepsilon_a)] = \tfrac{1}{2} f^{\gtrless}(\varepsilon_a). \tag{B17}$$

In the general case, the energy levels will vary with time. In order to investigate this case, we assume a linear shift of ε_a with distance and a uniform velocity. For this model, Λ takes the form

$$\Lambda(t,\bar{t}) = b\left(Z_0 - Z_c + \frac{v}{2}(t+\bar{t})\right)(t-\bar{t}) . \tag{B18}$$

This expression is inserted in Eq. (B14) and the following integral results:

$$\int_{-\infty}^{t} d\bar{t}\,\mathrm{Re}[\tilde{f}^{\gtrless}(t,\bar{t})]$$

$$= \tfrac{1}{4} \pm \tfrac{1}{2}\int_{-\infty}^{0} dx\,\frac{\sin\{[(b(Z-Z_c)+\frac{1}{2}bvx]x\}}{\beta\sinh(\pi x/\beta)} . \tag{B19}$$

The hyperbolic sine term in the denominator again provides a natural cutoff at $x = \beta/\pi$. The x^2 term in the argument of the sine term in the numerator can be neglected if

$$(Z-Z_c) \gg \frac{v}{2\pi}\beta . \tag{B20}$$

This condition defines a crossing time $\Delta t_c = \beta/\pi$ during which negligible charge transfer must be required, i.e., $\Gamma(t_c)\beta/2\pi \ll 1$. This is a special case of the criterion Eq. (B9) presented earlier. If the x^2 term in the argument for the sine term can be neglected, the resulting integration can directly be performed and the results are

$$\int_{-\infty}^{t} d\bar{t}\,\mathrm{Re}[\tilde{f}^{\gtrless}(t,\bar{t})] = \tfrac{1}{2} f^{\gtrless}(\varepsilon_a(t)) . \tag{B21}$$

For the SCA to be valid, it suffices that only one of the criteria Eq. (B9) or Eq. (B10) be satisfied. The conditions on velocity and temperature presented in this appendix are unnecessarily restrictive. Numerical studies of the corrections c(t) and $d^{\gtrless}(t)$ reveal a much broader applicability of the SCA than what has been indicated. In particular a good convergence at even zero temperature is obtained by the local approximation. This is most likely due to the fact that the numerator in the expression for $\tilde{f}^{\gtrless}$ oscillates with time and that even the modest t^{-1} cutoff provided by the denominator in the $T = 0$ K limit suffices to provide a localization. Nevertheless, the criteria presented here are satisfied in typical atom-surface-scattering experiments at room temperature. For a K atom with a kinetic energy of 1 eV, impinging at 45°, the perpendicular velocity is around $v = 0.0005$ a.u. At room temperature $\beta = 1000$. At a distance of 10 a.u. from the surface, the width is around 0.001 a.u. and $\alpha = 1.0$.[3] We thus see that the conditions in Eq. (B9) are both satisfied. If we assume that the level shift is due to the image potential, b=0.003, so also the second criterion Eq. (B10) is satisfied, although this would not be required for the validity of the SCA. For larger velocities Eq. (B10) will still apply. For smaller velocities Eq. (B9) will apply instead.

The above discussion assumes a planar surface so that the shifts of the atomic energy levels are smooth. Recently it has been shown in the $U = 0$ limit,[3] that in the presence of a lateral corrugation of atomic levels outside a surface and a nonperpendicular scattering geometry the

charge transfer occurs as if the electrons in the conduction band were characterized by a higher temperature. The analysis showed that the same type of localization that is induced by the hyperbolic sine term in the Dyson equations, results from such a corrugation. Application to ion-surface-scattering experiments revealed that the effective surface electron temperature was at least 2400 K. Most likely, the same result will apply also to the large-U limit, and sufficient localization is obtained from the criteria Eq. (B9) alone even for very broad levels. More work along these lines is clearly required before a definite assessment of the validity of the SCA for the description of charge-transfer processes between atoms and corrugated surfaces can be made.

APPENDIX C: SEMICLASSICAL APPROXIMATION FOR THE ADVANCED AND RETARDED GREEN'S FUNCTIONS

In this appendix, the approximations used to derive the expressions for the retarded and advanced Green's functions used for the evaluation of the correction terms for the master equation for large U are discussed. Due to the necessity of including both the real and imaginary parts of $\tilde{f}^{\gtrless}$ we follow a slightly different route than before.

The Dyson equation for the retarded Green's functions have the form

$$
\begin{aligned}
i\frac{\partial}{\partial t}\tilde{G}_\sigma^R(t,t') &= \delta(t-t') + \int_{-\infty}^{\infty} d\bar{t}\,\sqrt{\Gamma_\sigma(t)\Gamma_\sigma(\bar{t})}\,\tilde{f}_\sigma^{>}(t,\bar{t})B^R(t,\bar{t})\tilde{G}_\sigma^R(\bar{t},t')\ , \\
i\frac{\partial}{\partial t}B^R(t,t') &= \delta(t-t') + \sum_\sigma \int_{-\infty}^{\infty} d\bar{t}\,\sqrt{\Gamma_\sigma(t)\Gamma_\sigma(\bar{t})}\,\tilde{f}_\sigma^{<}(\bar{t},t)\tilde{G}_\sigma^R(t,\bar{t})B^R(\bar{t},t')\ .
\end{aligned}
\tag{C1}
$$

The imaginary part of $\tilde{f}^{\gtrless}(t,t')$ will result in a shift of the bare impurity levels. This shift introduces a new time dependence of the phase of the advanced and retarded Green's functions. We will here demonstrate that under certain circumstances, this shift can be neglected.

The real and imaginary parts of $\tilde{f}^{\gtrless}(t,t')$ are strongly peaked at $t = t'$ (in the infinite-band limit, Im$\tilde{f}$ diverges as $[\sinh \pi(t-t')/\beta]^{-1}$ and for the finite band the imaginary part will be localized within a time interval $\delta t = 1/D$). The SCA can thus be performed as usual and the following equations result:

$$
\begin{aligned}
i\frac{\partial}{\partial t}\tilde{G}_\sigma^R(t,t') &= \delta(t-t') \\
&\quad -i\Gamma_\sigma(t)\tilde{G}_\sigma^R(t,t')\int_{t'}^{t} d\bar{t}\,\tilde{f}_\sigma^{>}(t,\bar{t})\ , \\
i\frac{\partial}{\partial t}B^R(t,t') &= \delta(t-t') \\
&\quad -i\sum_\sigma \Gamma_\sigma(t)B^R(t,t')\int_{t'}^{t} d\bar{t}\,\tilde{f}_\sigma^{<}(\bar{t},t)\ .
\end{aligned}
\tag{C2}
$$

These expressions can of course directly be solved exactly, since $\tilde{f}^{\gtrless}$ only depend on $\varepsilon_\sigma(t)$ and the substrate parameters. In the present application, we content ourselves with only obtaining a qualitative estimate of the correction terms. To this end, we need approximate expressions for $\tilde{G}_\sigma^R(t,t')$ and $B_\sigma^R(t,t')$ valid in the limit of large and small $|t-t'|$. For $|t-t'| > \beta/\pi$, the integration over $\bar{t}$ in Eq.(C2) can be done from $t' = -\infty$. For simplicity we assume a constant level energy and a rectangular band of width 2D.

Using Eqs. (2.14) and (3.2), the following result is obtained:

$$
\begin{aligned}
\int_{-\infty}^{t} d\bar{t}\,\tilde{f}_\sigma^{\gtrless}(\bar{t},t) &= \int_{-\infty}^{t} d\bar{t}\,\exp[i\varepsilon_\sigma(t)(t-\bar{t})] \\
&\quad \times \int_{-D}^{D}\frac{d\varepsilon}{2\pi} f^{\gtrless}(\varepsilon)\exp[-i\varepsilon(t-\bar{t})]\ .
\end{aligned}
\tag{C3}
$$

The time integration can here be performed directly to yield

$$
\int_{-\infty}^{t} d\bar{t}\,\tilde{f}_\sigma^{\gtrless}(\bar{t},t) = \int_{-D}^{D}\frac{d\varepsilon}{2\pi} f^{\gtrless}(\varepsilon)\frac{-1}{i[\varepsilon_\sigma(t)-\varepsilon+i\eta]}\ ,
\tag{C4}
$$

where η is a real infinitesimal.

Using Cauchy's theorem, the following expressions are obtained:

$$
\int_{-\infty}^{t} d\bar{t}\,\tilde{f}_\sigma^{\gtrless}(\bar{t},t) = \frac{f^{\gtrless}(\varepsilon_\sigma(t))}{2} + iP\int_{-D}^{D}\frac{d\varepsilon}{2\pi}\frac{f^{\gtrless}(\varepsilon)}{\varepsilon_\sigma-\varepsilon}\ .
\tag{C5}
$$

These expressions can be inserted in Eq. (C2) and the equations can directly be solved. If the imaginary parts of $\tilde{f}^{\gtrless}$ are denoted by $P_\sigma^{\gtrless}(t)$, the retarded and advanced Green's functions can directly be obtained:

$$
\begin{aligned}
\tilde{G}_\sigma^R(t,t') &= -i\Theta(t-t')\exp\left(-\int_{t'}^{t} d\tau\,\frac{\Gamma_\sigma(\tau)}{2}f^{>}(\varepsilon_\sigma(\tau))\right)\exp\left(i\int_{t'}^{t} d\tau\,\frac{\Gamma_\sigma(\tau)}{2}P_\sigma^{>}(t)\right)\ , \\
B^R(t,t') &= -i\Theta(t-t')\exp\left(-\int_{t'}^{t} d\tau\,\sum_\sigma\frac{\Gamma_\sigma(\tau)}{2}f^{<}(\varepsilon_\sigma(\tau))\right)\exp\left(-i\int_{t'}^{t} d\tau\,\sum_\sigma\frac{\Gamma_\sigma(\tau)}{2}P_\sigma^{<}(t)\right)\ .
\end{aligned}
\tag{C6}
$$

For a wide band, the functions $P_\sigma^{\gtrless}(t)$ behave approximately as

$$P_\sigma^{\gtrless}(t) \approx \frac{1}{2\pi} \ln \left| \frac{\varepsilon_\sigma(t) - \varepsilon_F}{D} \right| . \quad \text{(C7)}$$

This correction can be neglected if the time integral is small over the time interval $\Delta t = \beta/\pi$ which contributes to the integrals in Eq. (3.17). We thus require

$$\Gamma_\sigma P_\sigma^{\gtrless} \frac{\beta}{\pi} \ll 1 . \quad \text{(C8)}$$

This above condition defines a required minimum energy separation between ε_σ and the Fermi energy:

$$|\varepsilon_\sigma - \varepsilon_F| \gg D \exp\left(-\frac{2\pi^2}{\beta\Gamma_\sigma}\right) . \quad \text{(C9)}$$

In the case with a level crossing, this criterion is equivalent to a crossing time:

$$\Delta t = \frac{D}{bv} \exp\left(-\frac{2\pi^2}{\beta\Gamma_\sigma}\right) . \quad \text{(C10)}$$

During this time we must require that only small charge transfer occur, i.e.,

$$\Gamma_\sigma(t_c) \left(\frac{D}{bv}\right) \exp\left(-\frac{2\pi^2}{\beta\Gamma_\sigma(t_c)}\right) \ll 1 . \quad \text{(C11)}$$

This criterion is satisfied in typical atom-surface collisions. The phase factor in Eq. (C6) will therefore be be neglected in the following. The SCA thus yields the following approximate expressions for the retarded Green's functions.

$$\tilde{G}_\sigma^R(t,t') = -i\Theta(t-t') \exp\left(-\int_{t'}^{t} d\tau \frac{\Gamma_\sigma(\tau)}{2} f^{>}(\varepsilon_\sigma(\tau))\right) , \quad \text{(C12)}$$

$$B^R(t,t') = -i\Theta(t-t') \times \exp\left(-\int_{t'}^{t} d\tau \sum_\sigma \frac{\Gamma_\sigma(\tau)}{2} f^{<}(\varepsilon_\sigma(\tau))\right) .$$

We note that these expressions are correct for $t \approx t'$ and for $t - t' \gg \beta/\pi$.

[1] D. M. Newns, Comments Cond. Mat. Phys. **14**, 295 (1989).
[2] P. D. Johnson, A. J. Viescas, P. Nordlander, and J. C. Tully, Phys. Rev. Lett. **64**, 942 (1990).
[3] P. Nordlander and J. C. Tully, Surf. Sci. **211**, 207 (1989).
[4] A. Blandin, A. Nourtier, and D. Hone, J. Phys. (Paris) **37**, 365 (1976).
[5] J. C. Tully, Phys. Rev. B **16**, 4324 (1977).
[6] J. K. Nørskov and B. I. Lundqvist, Phys. Rev. B **19**, 5661 (1979).
[7] R. Brako and D. M. Newns, Surf. Sci. **108**, 253 (1981).
[8] N. D. Lang, Phys. Rev. B **27**, 2019 (1983).
[9] W. Bloss and D. Hone, Surf. Sci. **72**, 277 (1978).
[10] T. B. Grimley, V. C. J. Bhasu, and K. L. Sebastian, Surf. Sci. **124**, 305 (1983).
[11] R. Brako and D. M. Newns, Solid State Commun. **55**, 633 (1985).
[12] K. L. Sebastian, Phys. Rev. B **31**, 6976 (1985).
[13] R. Brako and D. M. Newns, Rep. Prog. Phys. **52**, 655 (1989).
[14] P. Coleman, Phys. Rev. B **29**, 3035 (1984).
[15] L. P. Kadanoff and G. Baym, *Quantum Statistical Mechanics* (Benjamin, New York, 1962).
[16] D. C. Langreth, in *Linear and Nonlinear Electron Transport in Solids*, edited by J. T. Devreese and V. E. van Doren (Plenum, New York, 1976).
[17] L. V. Keldysh, Zh. Eksp. Teor. Fiz. **47**, 1515 (1964) [Sov. Phys. JETP **20**, 1018 (1965)].
[18] D. C. Langreth and J. W. Wilkins, Phys. Rev. **6**, 3189 (1972).
[19] J. J. C. Geerlings, J. Los, J. P. Gauyacq, and N. M. Temme, Surf. Sci. **172**, 257 (1986).
[20] P. Nordlander and J. C. Tully, Phys. Rev. B **42**, 5564 (1990).
[21] P. Nordlander and J. C. Tully, Phys. Rev. Lett. **61**, 990 (1988).
[22] M. J. Vasile, Phys. Rev. B **29**, 3785 (1984).